THEORETICA CHIMICA ACTA

Theoret. Chim. Acta (Berl.) 47, 111–131 (1978)

A MO-Theoretical Study of the Hydrogen Bond in $(HCOOH)_2$, $(HCONH_2)_2$ and $(B(OH)_3)_2$

Shinichi Yamabe

Department of Chemistry, Nara University of Education, Takabatake-cho, Nara, 630, Japan

Kazuo Kitaura and Kichisuke Nishimoto

Department of Chemistry, Osaka City University, Sumiyoshi-ku, Osaka, 558, Japan

The energy decomposition scheme is used with the *ab initio* MO of the STO-3G minimal basis to elucidate the nature of hydrogen-bondings in $(HCOOH)_2$, $(HCONH_2)_2$ and $(B(OH)_3)_2$. The comparison of the interaction energy and its five components, together with that of the difference density map, reveals the similarity or the difference of these three systems. Each component of the global difference density represents the characteristic role of the corresponding interaction. While the effect of the exchange and charge-transfer interaction is limited to the hydrogen-bonded region, that of the polarization and the coupling terms is spread over the intramolecular bonds of each monomer. The analysis of some orbital interactions is made with respect to $(HCOOH)_2$ and the importance of the particular charge-transfer interaction is demonstrated.

Key words: Energy decomposition – Hydrogen bond – Formic acid dimer – Formamide dimer – Orthoboric acid dimer

1. Introduction

Up to now, the *ab initio* SCF MO calculations have been extensively carried out for a wide variety of hydrogen bond (H-bond) systems. The most typical way to deal with the H-bond is the calculation of the supermolecule, including all constituent monomers [1]. Through this method, the H-bond energy and the global change of the charge distribution can be evaluated in comparison with the electronic quantity of the monomer calculated independently. Since H-bond systems have usually very weak interaction of (X–H···Y) type, the deviation of the electronic structure of the supermolecule from that of constituent monomers is small. This makes the discussion of the H-bond property in terms of the monomer electronic structure intuitively graspable. Taking advantage of this, the perturbation approach which gives a more chemically appealing feature than the supermolecule-calculation was

0040–5744/78/0047/0111/$04.20

put forth [2]. But, of course, this method is only applicable to the region where the interaction between monomers is sufficiently weak to be dealt with by the perturbation. To take up the merits of two methods, i.e., the accuracy of the supermolecule-calculation and the chemically understandable representation of the H-bond interaction of the perturbation approach, the energy decomposition scheme [3] and the configuration analysis [4] were proposed. Recently, the former technique has been given a solid theoretical ground [5] and its application to the donor-acceptor complexes which are of the stronger interaction than the H-bond has been made [6]. By this scheme, the total interaction energy (ΔE) is partitioned into five terms, i.e., electrostatic (E_{ES}), exchange (E_{EX}), polarization (E_{PL}), charge transfer (E_{CT}) and coupling (E_{MIX}) energies. Each term has a clear physical meaning. E_{ES} is the classical Coulombic energy between the undeformed electronic clouds of two monomers. E_{EX} is the repulsion energy due to the overlap of the doubly occupied MO's. E_{PL} is the stabilization energy due to the mixing in of the intramolecular excited configuration. E_{CT} is the stabilization energy due to the contribution of the charge-transferred configuration from the occupied (occ) MO of one monomer to the vacant (vac) one of the other and *vice versa*. E_{MIX} is the residual term after E_{ES}, E_{EX}, E_{CT} and E_{PL} are subtracted from ΔE and is the sum of "cross terms" between the above defined four components. As the extension of the energy decomposition scheme, the electron distribution can be also analyzed according to the type of each interaction.

The cyclic dimers such as formic acid dimer are known to have the two H-bonds [7]. Clementi and his coworkers discussed whether the double well potential appears through the proton movement or not [8]. It is a matter of the biochemical importance to investigate how the two H-bonds interact with each other. In order to understand the nature of the two H-bonds in cyclic dimers from a unified point of view, we shall make a comparative study of three systems, i.e., the formic acid dimer, $(HCOOH)_2$, the formamide dimer, $(HCONH_2)_2$ and the orthoboric acid dimer, $(B(OH)_3)_2$, by the use of the energy decomposition scheme. In addition to the way of calculation introduced above, we shall here extend it further to the analysis of the MO–MO interaction and clarify the nature of the H-Bond in the MO language. In this work, our attention is also paid to the similarity and the difference of the nature of three cyclic dimers through the study of the density distribution.

In Sect. 2, the derivation of the energy decomposition scheme is briefly reviewed together with some additional comments. In Sect. 3, the details of the calculation (e.g., the geometry of three systems) is stated. In Sect. 4, the result of interaction energies and the contour map of the electron density are presented. In Sect. 5, the conclusive discussion is given especially with regard to the point of how two H-bonds interact with each other in the cyclic dimer.

2. Review of the Energy Decomposition Scheme

Consider a system (or supermolecule) consisting of two monomers, A and B. It is assumed that both A and B have the closed-shell electronic configuration in the ground state which is suitably described by the Hartree–Fock (HF) MO obtained

independently in two monomers. Then the electronic structure of the system is represented by the orbital interaction of MO's of A and B. As shown later, the degree and the mode of the orbital interaction are ascribed to the way of the choice of corresponding matrix elements on the basis of these MO's in the isolated state of A and B, respectively. In this sense, they constitute the zeroth order wavefunction for the interacting system. The HF equation of the supermolecule is written as follows:

$$(\boldsymbol{F} - \varepsilon \boldsymbol{S})\boldsymbol{C} = 0 \tag{1}$$

$\boldsymbol{F}$ is the Fock matrix, $\boldsymbol{S}$ is the overlap matrix, $\boldsymbol{C}$ is the coefficient matrix, and ε is the orbital energy. When the total energy of the supermolecule obtained by solving Eq. (1) is subtracted by that of A and B, one can get the interaction energy, ΔE. According to the physical picture, ΔE is partitioned into various components in the following way. The interaction matrix, $\boldsymbol{\Sigma}$, is defined in Eq. (2).

$$\boldsymbol{\Sigma} = (\boldsymbol{F} - \varepsilon \boldsymbol{S}) - (\boldsymbol{F}^0 - \varepsilon \boldsymbol{1}) \tag{2}$$

$\boldsymbol{F}^0$ is the Fock operator at the infinite separation, being composed of Fock operator of A and B in their isolated state and it does not have the off-diagonal matrix element. The matrix, $\boldsymbol{\Sigma}$, defined in such a way has the role to cause the intermolecular or intramolecular interaction of MO's. $\boldsymbol{\Sigma}$ is decomposed into the following six components.

$$\boldsymbol{\Sigma} = \boldsymbol{\Sigma}^{\mathrm{ES(X)}} + \boldsymbol{\Sigma}^{\mathrm{EX'}} + \boldsymbol{\Sigma}^{\mathrm{PL(X)A}} + \boldsymbol{\Sigma}^{\mathrm{PL(X)B}} + \boldsymbol{\Sigma}^{\mathrm{CT(A\rightarrow B)}} + \boldsymbol{\Sigma}^{\mathrm{CT(B\rightarrow A)}} \tag{3}$$

Eq. (3) can be described pictorially as follows.

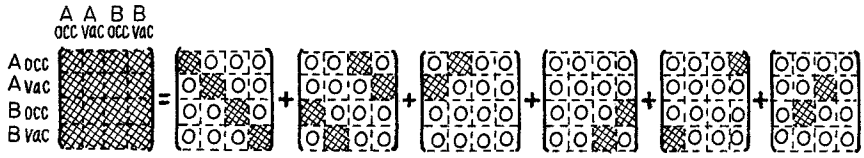

$\boldsymbol{\Sigma}^{\mathrm{CT(A\rightarrow B)}}$ is, for example, a matrix with the partial matrix element of $\boldsymbol{\Sigma}$, including blocks of the occupied MO's of A and unoccupied ones of B and is regarded as the origin to bring about the charge transfer (CT) interaction (A → B). The notations, ES(X), PL(X)A and PL(X)B attached to the right shoulder of the first, third and fourth terms mean the electrostatic, the polarization of A and the polarization of B, respectively, with some additional molecular integrals related simultaneously to both A and B. When these molecular integrals which are usually of small value are omitted by the intermolecular zero differential overlap, these three terms are reduced to those of the traditional electrostatic and the polarization of A and B. Once $\boldsymbol{\Sigma}$ is partitioned into six terms with its different shaded blocks, the pseudo HF equation which picks up only one (or a few) term(s) from the interaction matrix, $\boldsymbol{\Sigma}$, is given as follows.

$$\{(\boldsymbol{F}^0 - \varepsilon \boldsymbol{1}) + \boldsymbol{\Sigma}^x\}\boldsymbol{C}^x = 0 \tag{4}$$

Then, each energy component of the global interaction energy (ΔE) is derived by the use of the solution of Eq. (4). When $x = \mathrm{ES(X)} + \mathrm{CT(A \rightarrow B)}$ in Eq. (4), the resultant total energy is, say $E^{\mathrm{ES(X)+CT(A \rightarrow B)}}$, which contains the effect of the electrostatic (ES), a part of the exchange interaction (X) and the CT interaction from A to B. Another pseudo HF equation with $x = \mathrm{ES(X)}$ is solved, the net (A → B) CT interaction energy is easily obtained by the difference between two energies.

In this work, the negative value of any energy term denotes the stabilization component. Other components of ΔE can be obtained similarly by taking the appropriate blocks of Σ. According to the original definition, ΔE is represented by the sum of five terms which are already introduced in the previous section

$$\Delta E = E_{\mathrm{ES}} + E_{\mathrm{EX}} + E_{\mathrm{PL}} + E_{\mathrm{CT}} + E_{\mathrm{MIX}}. \tag{5}$$

For the planar system, ΔE is further divided into π and σ parts

$$\Delta E = E_{\mathrm{ES}} + E_{\mathrm{EX}}^{\sigma} + E_{\mathrm{EX}}^{\pi} + E_{\mathrm{PL}}^{\sigma} + E_{\mathrm{PL}}^{\pi} + E_{\mathrm{CT}}^{\sigma} + E_{\mathrm{CT}}^{\pi} + E_{\mathrm{MIX}}. \tag{6}$$

It should be noted that E_{PL} and E_{CT} are twice as large as the "one-sided" polarization and CT energies, respectively. That is, E_{PL} does not include the effect of the simultaneous polarization in both monomers, nor does E_{CT} include that of the mutual CT (i.e., donation and back donation) interaction. Such coupling effects of higher order are put together into E_{MIX}. Later, the energy difference between the presence and the absence of these configurations will be examined.

In addition to such a well established way of expressing ΔE, the extension of this method can be made by analyzing the block of Σ more precisely. Since each block is represented by the matrix elements in terms of individual MO's, one can partition the energy component into terms of *particular* orbital interaction [9]. For example, the (A → B) CT interaction energy can be divided into π and σ parts in the case of the planar supermolecule.

$$\Sigma^{\mathrm{CT(A \rightarrow B)}} = \Sigma^{\mathrm{CT(A \rightarrow B)}}(\pi) + \Sigma^{\mathrm{CT(A \rightarrow B)}}(\sigma) \tag{7}$$

The behaviour of the CT interaction from the highest occupied MO of A to the lowest unoccupied one of B which is the important combination to study the reactivity [10] can be also investigated. The decomposition of the electronic redistribution corresponding to each term of ΔE is also feasible, while the analysis of the interaction energy, ΔE, can be made as detailed as desired. When the pseudo HF equation of Eq. (4) is solved, the pseudo MO containing the effect of the interaction, x, can be obtained. By the use of the first order spinless density matrix [11] constructed by MO's, the density map can be drawn. Thus, the deformation of the electronic cloud due to the inclusion of the (A → B) CT interaction is represented by the following difference density, $\Delta\rho(1|1)_{\mathrm{CT(A \rightarrow (B)\varepsilon}}$.

$$\Delta\rho(1 \mid 1)_{\mathrm{CT(A \rightarrow B)}} = \rho(1 \mid 1)_{\mathrm{CT(A \rightarrow B)}} - \{\rho(1 \mid 1)_{\mathrm{A}} + \rho(1 \mid 1)_{\mathrm{B}}\} \tag{8}$$

Thus, the difference density, $\Delta\rho(1 \mid 1)$, due to the H-bond formation is described as follows:

$$\Delta\rho(1 \mid 1) = \Delta\rho(1 \mid 1)_{EX} + \Delta\rho(1 \mid 1)_{PL(A)} + \Delta\rho(1 \mid 1)_{PL(B)} + \Delta\rho(1 \mid 1)_{CT(A\to B)} + \Delta\rho(1 \mid 1)_{CT(B\to A)} + \Delta\rho(1 \mid 1)_{MIX}. \quad (9)$$

Eq. (9) corresponds just to Eq. (5) except the omission of "$\Delta\rho(1 \mid 1)_{ES}$". The electrostatic interaction has no effect on the deformation of the electronic cloud. If the H-bond system is planar, $\Delta\rho(1 \mid 1)$ can be divided furthermore into σ and π parts

$$\begin{aligned}\Delta\rho(1 \mid 1) &= \Delta\rho(1 \mid 1)^{\sigma} + \Delta\rho(1 \mid 1)^{\pi} \\ &= \Delta\rho(1 \mid 1)^{\sigma}_{EX} + \Delta\rho(1 \mid 1)^{\pi}_{EX} + \Delta\rho(1 \mid 1)^{\sigma}_{PL(A)} + \Delta\rho(1 \mid 1)^{\pi}_{PL(A)} \\ &\quad + \Delta\rho(1 \mid 1)^{\sigma}_{PL(B)} + \Delta\rho(1 \mid 1)^{\pi}_{PL(B)} + \Delta\rho(1 \mid 1)^{\sigma}_{CT(A\to B)} \\ &\quad + \Delta\rho(1 \mid 1)^{\pi}_{CT(A\to B)} + \Delta\rho(1 \mid 1)^{\sigma}_{CT(B\to A)} + \Delta\rho(1 \mid 1)^{\pi}_{CT(B\to A)} \\ &\quad + \Delta\rho(1 \mid 1)^{\sigma}_{MIX} + \Delta\rho(1 \mid 1)^{\pi}_{MIX}.\end{aligned} \quad (10)$$

When the density map is drawn with respect to the molecular plane, the π component of the density does not appear due to its nodal property in the plane.

Yamabe and Morokuma studied the hydrogen bonded system with the single O···H–O bond in terms of the scheme different only trivially from the present one and demonstrated the characteristic role of each component of the global difference density [12]. In this work, the nature of each interaction is examined by the use of some hydrogen bonded systems with two O···H–O or O···H–N bonds, and the difference or the similarity between single and two hydrogen bonds is elucidated.

3. Details of Calculation

As an application of the method explained in the previous section, three cyclic dimers are adopted. To evaluate the electronic structure of them, the MO is calculated with the STO-3G minimal basis set of the standard parametrization [13]. For this purpose, the FORTRAN program GAUSSIAN 70 [14] is used after some modifications for FACOM 230-75 computer are made, and the additional part of the program for the energy decomposition is incorporated into the original version of Kitaura and Morokuma [5]. The advantage and the disadvantage of this small basis set have already been examined [15, 19] and the trend of the obtained result with the larger basis set is conceivable without performing the calculation. For example, the small basis set such as the minimal STO-3G gives the small E_{ES} and the large E_{CT}. On the other hand, the extended basis set such as the 4-31G gives the opposite trend. Since five components of ΔE in Eq. (5), thus, significantly depend on the choice of the basis sets, even the order of their calculated values is unreliable. Considering this basis set dependency, we are not nervous about their absolute values, but we concentrate our attention on the comparisons of three H-bonded systems. In order to keep the chemically understandable picture, we confine ourselves to the minimal basis set throughout this work.

The geometry of three H-bond systems is taken from experimental data [7, 18, 20]. Although it is more desirable to obtain the optimized geometry by the same basis set as is used in the energy decomposition (STO-3G, minimal), it takes much computer time for $(B(OH)_3)_2$. Fortunately, the small basis set is thought to reproduce the experimental geometries to a satisfactory extent [16]. The adopted experimental geometries are shown in Fig. 1. The formic acid dimer was elaborately studied by Clementi and his coworkers, and the probability that the simultaneous movement of two hydrogen atoms along the O–H···O line results in a multiminimal well is pointed out [8]. Del Bene and Kochenour obtained the STO-3G optimized geometry of the formic acid dimer, showing the good agreement with the experimental one except for a minor underestimation of the intermolecular O···O distance. Recently, Iwata and Morokuma investigated the excited states of $(HCOOH)_2$ through the use of the TCEHP method [17]. In order to carry out the energy decomposition scheme, we use the one fragmental site of the dimer geometry as the monomer structure, which is somewhat different from the experimental monomer HCOOH geometry [21]. For the formamide dimer, Pullman and her coworkers [19] reported the SCF calculation, using the geometry determined by the X-ray diffraction experiment. They investigated mainly the change of the electron distribution upon the dimer formation. We here use the same geometry as that adopted by them. The crystal structure of orthoboric acid (H_3BO_3) is determined by neutron diffraction analysis [20]. In the crystal, monomers are linked together by O–H···O bonds to form the endless layers of nearly hexagonal symmetry. Each

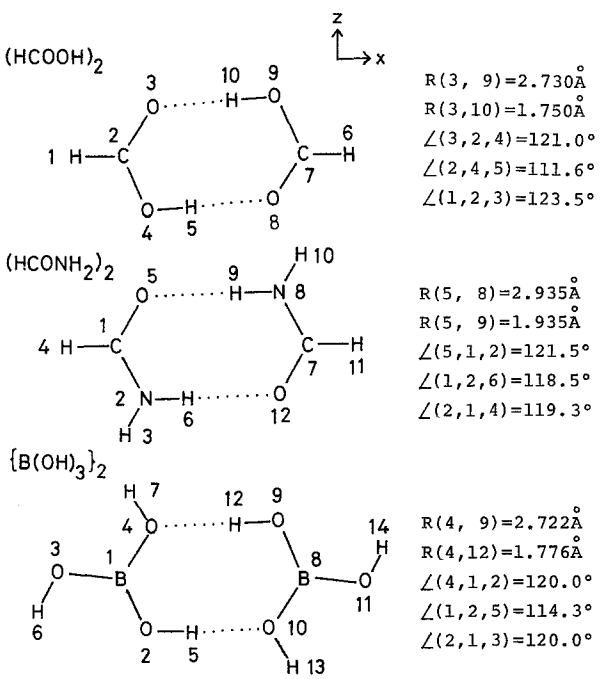

Fig. 1. Geometries of the three cyclic dimers. These are taken from the experimental data. The monomers located at the left-hand side are called A and those at the right-hand side are called B throughout the text

layer is stacked one by one with the separation of 3.181 Å. No theoretical study has been made as to this system, because it has the infinite linkage of $B(OH)_3$ units. Since each monomer is linked in the form of the cyclic dimer, we tentatively simplify the $B(OH)_3$ crystal structure as the dimer system. For the dimer geometry, we use the experimental value, neglecting the small nonplanarity of each layer due to the plane–plane interaction.

Since all constituent atoms of three H-bonded systems are located in a plane, the density map will be pictured in the same plane. The π electron distribution which cannot be shown by the density map will be demonstrated by the Mulliken population analysis.

4. Result of Calculation

In Table 1, the calculated interaction energies are shown with respect to three cyclic H-bonded systems. Let us concentrate our attention on each term of the $(HCOOH)_2$ system. The global H-bond energy, ΔE, is calculated to be -15.65 kcal/mole, which is, of course, very similar to the result of Del Bene and Kochenour (-15.1 kcal/mole) with their fully optimized geometry [17]. The experimental ΔE is -14.8 ± 0.5 kcal/mole [22]. Five components of ΔE are characteristic of the H-bonded system. Among them, the combination of E_{EX} (22.94 kcal/mole) and E_{CT} (-20.56 kcal/mole) shows good compensation, which is reasonable in consideration of the fact that both terms are of second order of the MO overlap in the perturbation sense [23]. E_{ES} is the third largest term among five and is comparable to ΔE. As far as this result is concerned together with that of $(B(OH)_3)_2$, the electrostatic approximation of the H-bond energy seems applicable to predict ΔE [24]. But obviously, this approximation cannot be applied to the $(HCONH_2)_2$ because ΔE (-15.19 kcal/mole) is quite different from E_{ES} (-10.92 kcal/mole). E_{PL} of $(HCOOH)_2$ is very small (-0.84 kcal/mole). This small value has been obtained in many systems [9] and seems a trifling component from the energetic point of view. But it has surprisingly the important role of rearranging the electronic distribution [12] as will be demonstrated later and consequently is far from the negligible one of informing the entire system of the H-bond effect. E_{MIX} is calculated

Table 1. The calculated interaction energy, ΔE, and its five components as to three cyclic dimers. They are obtained with the STO-3G minimal basis set by the use of the experimental geometries shown in Fig. 1. All the values are in kcal/mole and the negative value denotes the stabilization energy

	$(HCOOH)_2$	$(HCONH_2)_2$	$(B(OH)_3)_2$
ΔE	-15.65	-15.19	-14.16
E_{ES}	-14.35	-10.92	-14.31
E_{EX}	22.94	11.12	21.72
E_{PL}	-0.84	-0.76	-0.54
E_{CT}	-20.56	-13.56	-18.36
E_{MIX}	-2.84	-1.07	-2.77

to be the second smallest term, which gives one evidence that this type of H-bond is relatively of the weak interaction[1].

In order to see the contribution of the mutual CT interaction to E_{CT}, it is recalculated with the inclusion of this interaction and is found to be -20.66 kcal/mole. This value is almost the same as E_{CT} (-20.56 kcal/mole) in Table 1, which indicates that the coupling CT interaction is of much less importance than the one-sided CT interaction (i.e., $E_{CT} \simeq E_{CT(A\to B)} + E_{CT(B\to A)}$). In other words, the donation and back donation do not work cooperatively and their role can be treated independently in $(HCOOH)_2$. Similarly, E_{PL} is recalculated with the inclusion of the simultaneous polarization in both A and B (i.e., dispersion type) and is found to be -0.94 kcal/mole. This value is very close to E_{PL} (-0.84 kcal/mole) shown in Table 1, resulting in the validity of the independent description of the polarization interaction in each monomer.

Let us compare each component of three different H-bonded systems. Seeing three ΔE's in Table 1, one notices that ΔE of $(HCOOH)_2$ (-15.65 kcal/mole) is very close to that (-15.19 kcal/mole) of $(HCONH_2)_2$. This is apparently strange, because it has been believed that the O–H···O bond is stronger than the N–H···O H-bond. But, if we pay attention to each component of ΔE, the difference of the ability of H-bond formation between these two can be recognized. That is, each term of $(HCOOH)_2$ is much larger than that of $(HCONH_2)_2$ (e.g., 22.94 kcal/mole vs. 11.12 kcal/mole of E_{EX}). Thus, we may state that the apparent equivalence of ΔE in both systems is brought about by the accidental coincidence due to the different extent of the compensation between positive (E_{EX}) and the negative four terms. Comparing two ΔE's of $(HCOOH)_2$ and $(B(OH)_3)_2$, one finds more stabilization energy in the former system than in the latter, the difference being ~ -1.5 kcal/mole. This is somewhat strange, because both systems have almost the same O···O distance ($=2.73$ Å) and they are expected to give similar ΔE's. This difference is ascribed to E_{CT} (-20.56 vs. -18.36 kcal/mole). The superiority or inferiority of E_{CT}'s is due to the following reason. The gap of orbital energies between σ and σ^* MO's is smaller in the HCOOH monomer, which makes the electron jumping through σ-type MO's easy and consequently yields the larger stabilization energy, E_{CT} in $(HCOOH)_2$.

Now, let us investigate the electron density redistribution due to the H-bond formation. In Table 2, the Mulliken atomic population of an isolated HCOOH(A) and four kinds of the atomic net charge are exhibited. The first of these four is, for instance, the difference between the Mulliken atomic population under the influence of the one-sided polarization and that in the isolated state. Making comparisons [ΔN_α (one-sided polarization) vs. ΔN_α (simultaneous polarization) and ΔN_α (one-sided CT) vs. ΔN_α (mutual CT)], one finds that the difference between the corresponding two terms is very small. This result, together with the calculated one of E_{PL} and E_{CT}, demonstrates the usefulness of the employment of the one-sided polarization and CT interactions to define these two energetic terms.

[1] In general, when the molecular interaction becomes stronger, the coupling term, E_{MIX}, grows larger. See Ref. [6].

Table 2. The Mulliken atomic population of the atom α (N_α) and four kinds of the difference atomic population (ΔN_α) of HCOOH(A). The position and the numbering of the α-atom are indicated in Fig. 1. ΔN_α represents the fluctuation of the population due to the interaction shown in the parentheses. The negative value in the table means the decreased electron density

No.	α (Atom)	N_α (Isolated)	ΔN_α (One-sided polarization)	ΔN_α (Simultaneous polarization)	ΔN_α (One-sided CT)	ΔN_α (Mutual CT)
1	H	0.9153	−0.0038	−0.0039	−0.0011	−0.0011
2	C	5.7585	−0.0081	−0.0090	−0.0033	−0.0028
3	O	8.2520	0.0345	0.0390	−0.0427	−0.0436
4	O	8.2996	−0.0013	−0.0008	0.0030	0.0033
5	H	9.7746	−0.0213	−0.0253	0.0440	0.0442

Next, the change of the atomic orbital population of the monomer HCOOH(A) is shown in Table 3, according to the classification of four (exchange, polarization, CT and MIX) interactions. Since the detailed analysis of the σ electron rearrangement is made later by the contour map of the difference density, only the change of the π orbital charge is discussed. Taking a look at all the gross π orbital charges underlined in the table, we realize that the π electron moves toward the carbonyl oxygen, O(3), of the monomer A. This is because the O(3) faces the cationic hydrogen atom H(10) of the monomer B in the H-bonded geometry and consequently

Table 3. The Mulliken orbital population of the atomic orbital x (N_x) and four kinds of the difference orbital charge (ΔN_x) of HCOOH

α (Atom)	No.	x (Atomic orbital)	N_x (Isolated)	ΔN_x (Exchange)	ΔN_x (One-sided polarization)	ΔN_x (One-sided CT)	ΔN_x (MIX)
1	1	H(1s)	0.9153	0.0003	−0.0038	−0.0011	−0.0006
	2	C(1s)	1.9937	0.0000	0.0001	0.0000	0.0000
	3	C(2s)	1.1099	0.0002	0.0031	−0.0004	0.0042
2	4	C($2p_x$)	0.9650	0.0000	0.0047	−0.0005	0.0040
	5	C($2p_y$) π	0.9108	−0.0002	−0.0193	−0.0003	−0.0245
	6	C($2p_z$)	0.7793	0.0005	0.0032	−0.0021	0.0092
	7	O(1s)	1.9982	0.0000	0.0000	−0.0001	0.0000
	8	O(2s)	1.8765	0.0003	−0.0037	−0.0115	0.0007
3	9	O($2p_x$)	1.6942	−0.0005	0.0046	−0.0314	−0.0048
	10	O($2p_y$) π	1.2244	0.0001	0.0299	0.0003	0.0438
	11	O($2p_z$)	1.4584	0.0002	0.0040	0.0000	0.0049
	12	O(1s)	1.9975	0.0000	0.0000	0.0000	0.0000
	13	O(2s)	1.8066	0.0001	0.0010	−0.0001	−0.0022
4	14	O($2p_x$)	1.1949	0.0100	0.0174	0.0032	0.0475
	15	O($2p_y$) π	1.8648	0.0000	−0.0105	0.0000	−0.0192
	16	O($2p_z$)	1.4360	0.0001	−0.0094	−0.0001	−0.0137
5	17	H(1s)	0.7746	−0.0112	−0.0213	0.0440	−0.0492

that atom pulls the induced electron density through the mobile π route (see scheme). The gross π orbital charge in Table 3 reveals the important and cooperative role of the polarization and mixing term to cause the above mentioned movement of π electrons. The exchange and CT interactions have a negligible effect on the redistribution of π electrons, whereas they work significantly to rearrange σ electrons as shown later.

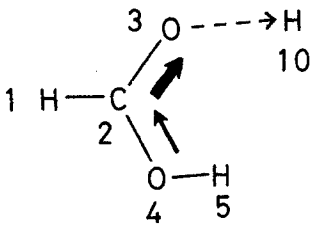

Let us proceed to the analysis of the density distribution of σ electrons. The density map of $(HCOOH)_2$ is pictured in Fig. 2. Five difference density maps, $\Delta\rho(1 \mid 1)$, $\Delta\rho(1 \mid 1)_{EX}$, $\Delta\rho(1 \mid 1)_{PL(A)}$, $\Delta\rho(1 \mid 1)_{CT(A\to B)}$ and $\Delta\rho(1 \mid 1)_{MIX}$ of Eq. (9) are drawn. In $\Delta\rho(1 \mid 1)$ of Fig. 2(a), we see the complex electron rearrangement over the whole system. But as far as the H-bond region of O···H–O is concerned, the density distribution is very similar to that of the system with the single O···H–O bond [12]. In Fig. 2(b), $\Delta\rho(1 \mid 1)_{EX}$ is shown to have the locality of the O···H–O bond and its effect is not transmitted around the cyclic dimer. The electron density which comes from the intermolecular region is piled up sharply on the sites of carbonyl oxygens and the H–O bonds. The locality of $\Delta\rho(1 \mid 1)_{EX}$ indicates that two O···H–O bonds do not couple through the exchange interaction. $\Delta\rho(1 \mid 1)_{PL(A)}$ is pictured as regards one monomer at the left side in Fig. 2(c). Thus, the polarized electron distribution under the influence of the partner monomer of the right side is shown. This $\Delta\rho(1 \mid 1)_{PL(A)}$ shows the typical trend that the electron density of the H-bonded hydrogen is decreased and that its effect is delocalized over the entire monomer, accompanying alternative appearance of the increase and decrease of the electron density through bonds of the monomer. Similar to systems with the single H-bond [12], the charge redistribution due to the polarization interaction is surprisingly large in spite of the small E_{PL}. In Fig. 2(d), the difference density due to the CT interaction from one monomer of the left side to that of the right side, $\Delta\rho(1 \mid 1)_{CT(A\to B)}$, is drawn. In this figure, the charge migration from the sp^2 lone pair orbital of O(3) of the electron-donating monomer to the H–O σ^* antibonding orbital of the electron-accepting one is clearly demonstrated. It should be noted that the appearance of the intermolecular bonding density is caused by this CT interaction. In addition, the ditch of the bonding density on the O–H bond of the electron acceptor arises from the nodal property of the O–H α^* antibonding orbital. As a whole, the effect of the CT interaction is transmitted *horizontally* along the O···H–O bond line and two CT interactions (i.e., donation and back donation) are distinguishable with the minor mixing between them. The separability of the donation and back donation is in accord with the energetic result that E_{ET} is well represented by being twice as large as the one-sided CT energy. The left

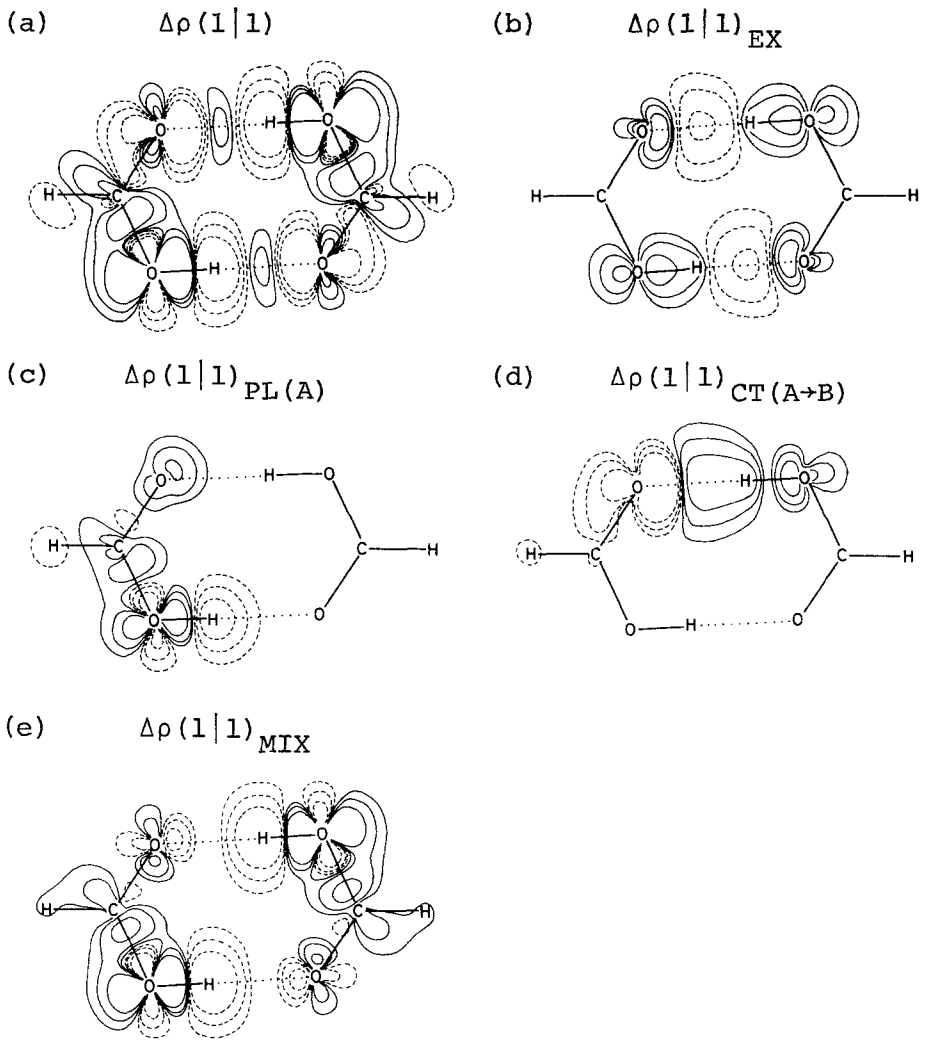

Fig. 2. The difference electron density of $(HCOOH)_2$. The full lines indicate density increases and dotted lines decreases. Values of these lines are, successively, ± 0.003, ± 0.008, ± 0.02 (e/Å^3)

half of the contour map of $\Delta\rho(1 \mid 1)_{MIX}$ in Fig. 2(e) is similar to that of $\Delta\rho(1 \mid 1)_{PL(A)}$. That is, the H-bonded proton loses the charge density considerably through this coupling term and the mode of the intramolecular charge alternation is close to that of $\Delta\rho(1 \mid 1)_{PL(A)}$. But the difference between $\Delta\rho(1 \mid 1)_{PL(A)}$ and $\Delta\rho(1 \mid 1)_{MIX}$ is found on the carbonyl oxygen atom, O(3). Whereas the charge density of O(3) along the H-bonded direction is decreased in the latter map, it is increased in the former, being induced by the "cationic" H-bonded proton of the partner monomer. Since E_{MIX} is the sum of all the coupling terms, its effect is difficult to interpret physically. But as far as the cyclic dimer of $(HCOOH)_2$ is concerned, the role of the mixing term is found in the remarkable charge redistribution of each monomer.

In spite of the small values of E_{MIX} and E_{PL}, their effects on the charge alternation in the intramolecular region are really noticeable.

Next, the difference density, $\Delta\rho(1\,|\,1)$ of three H-bonded systems is compared in Fig. 3. It is noted that these systems have very similar electron redistribution and

(a) $(HCOOH)_2$ $\Delta\rho(1|1)$

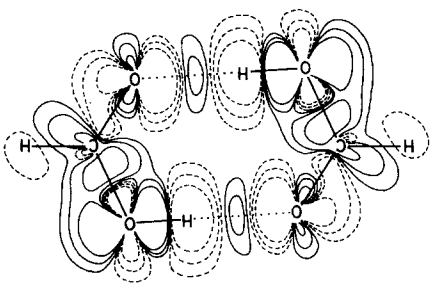

(b) $(HCONH_2)_2$ $\Delta\rho(1|1)$

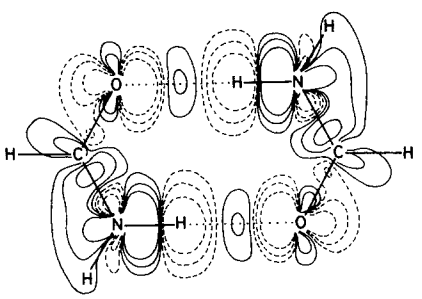

(c) $\{B(OH)_3\}_2$ $\Delta\rho(1|1)$

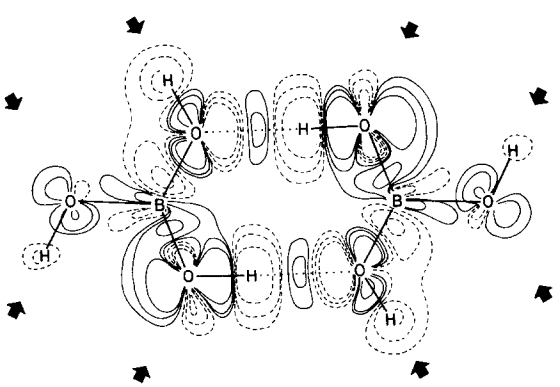

Fig. 3. The global difference electron density of $(HCOOH)_2$, $(HCONH_2)_2$ and $(B(OH)_3)_2$. The arrows in (c) indicate the direction of additional possible H-bonds. The scale of the contour lines is the same as that of Fig. 2

the mode of the charge alternation along the O···H–O and O···H–N is almost the same as in the systems with the single O···H–O bond [12]. Here, we focus our attention on $(B(OH)_3)_2$. The electronic structure of the $B(OH)_3$ monomer is of interest, because it forms electron-deficient bonds. The present *ab initio* SCF MO calculation reveals its following unique nature. In the σ-type B–O bond, the boron atom behaves as an electron donor, whereas in the π-type B–O bond which is described by the "four-center six-electron bond", the boron atom acts as an electron acceptor. Such a coexistence of the σ donating and π accepting of electrons in a chemical bond is a very interesting feature, especially when the participating atoms are confined to the hydrogen and first-row ones. In our calculation, we have assumed the dimer structure of orthoboric acid, but this dimer is actually surrounded by four orthoboric acids in the crystal structure. The present result of the difference density, $\Delta\rho(1 \mid 1)$, reveals the interesting feature of the hydroxyl groups in this assumed dimer. That is, the non-H-bonded hydrogen atoms lose the electron density somewhat and the oxygen atoms, O(2), O(3), O(9) and O(11) shown in Fig. 1, gain the electron density. This change of the electron distribution is to prompt the formation of H-bonds between the neighboring four $B(OH)_3$'s and the cyclic dimer (see the following scheme). In this way, the endless H-bonded layer might be formed in the $B(OH)_3$ crystal. In Figs. 4 to 6, $\Delta\rho(1 \mid 1)_{EX}$, $\Delta\rho(1 \mid 1)_{PL(A)}$ and $\Delta\rho(1 \mid 1)_{CT(A\to B)}$ are drawn so as to examine the effect of each interaction on the electron rearrangement in three systems. In these figures, the similarity or the difference among three systems is clearly revealed. The origin of the charge redistribution welcoming four surrounding $B(OH)_3$'s in the $(B(OH)_3)_2$ system is found

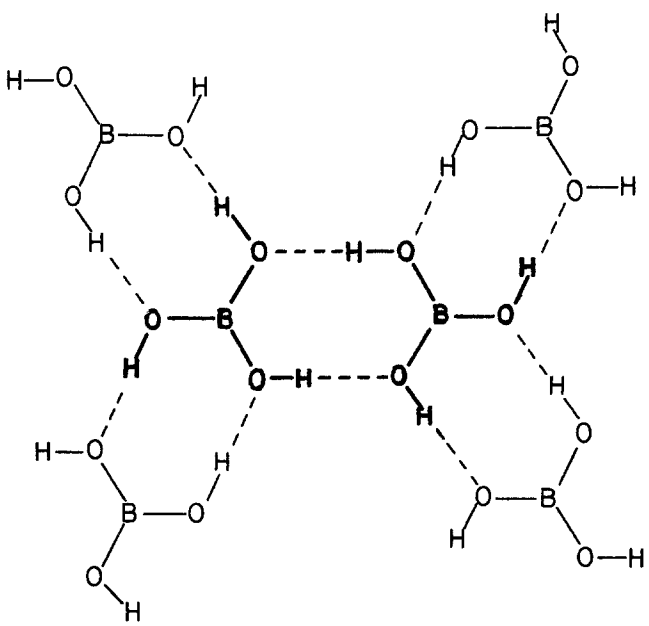

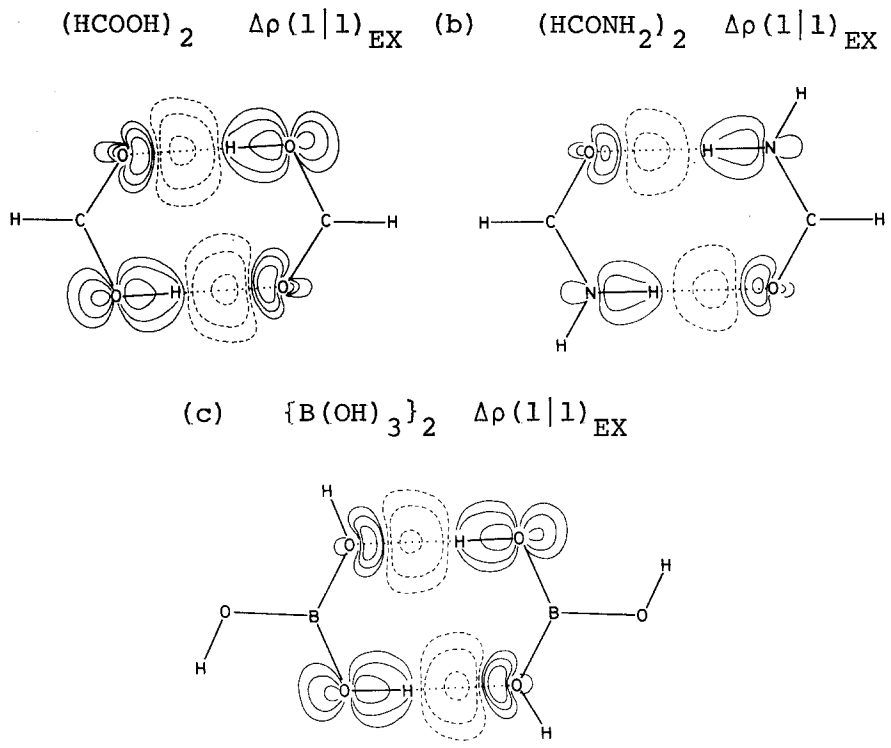

Fig. 4. The difference electron density due to the exchange repulsion interaction in $(HCOOH)_2$, $(HCONH_2)_2$ and $(B(OH)_3)_2$. See Fig. 2 for detail

in $\Delta\rho(1\,|\,1)_{PL(A)}$ and $\Delta\rho(1\,|\,1)_{MIX}$ (not shown). The effect of exchange and CT interaction is limited to each (O···H–O or O–H···O) H-bond. Thus, an important role of the polarization interaction is recognized in view of the mechanism of the endless H-bond formation of the orthoboric acid crystal.

So far, the H-bond energy, ΔE, has been investigated in terms of five components, among which E_{EX}, E_{CT} and E_{PL} are represented by the interaction of many pairs of MO's. For example, E_{EX} is the sum of all the exchange energies between doubly occupied MO's of two monomers. As for these terms, the analysis of the particular orbital interaction is performed with respect to $(HCOOH)_2$ system. This procedure is expected to give a better understanding of the mechanism of the H-bond formation. For this purpose, active occupied and unoccupied MO's which play a key role in causing some particular orbital interactions are taken up. The criterion to choose active MO's is the height of orbital energies. That is, the occupied MO is unstable (smaller ionization potential) and the unoccupied MO is eager to accept electron (larger electron affinity). In Fig. 7, orbital energies of two HCOOH monomers (A and B) are displayed, which are calculated again with the STO-3G minimal basis, where σ and σ^* are MO's within the x-z molecular plane (see Fig. 1) and π and π^* are along the y axis. Seeing Fig. 7, one can tentatively select $10(\sigma)$,

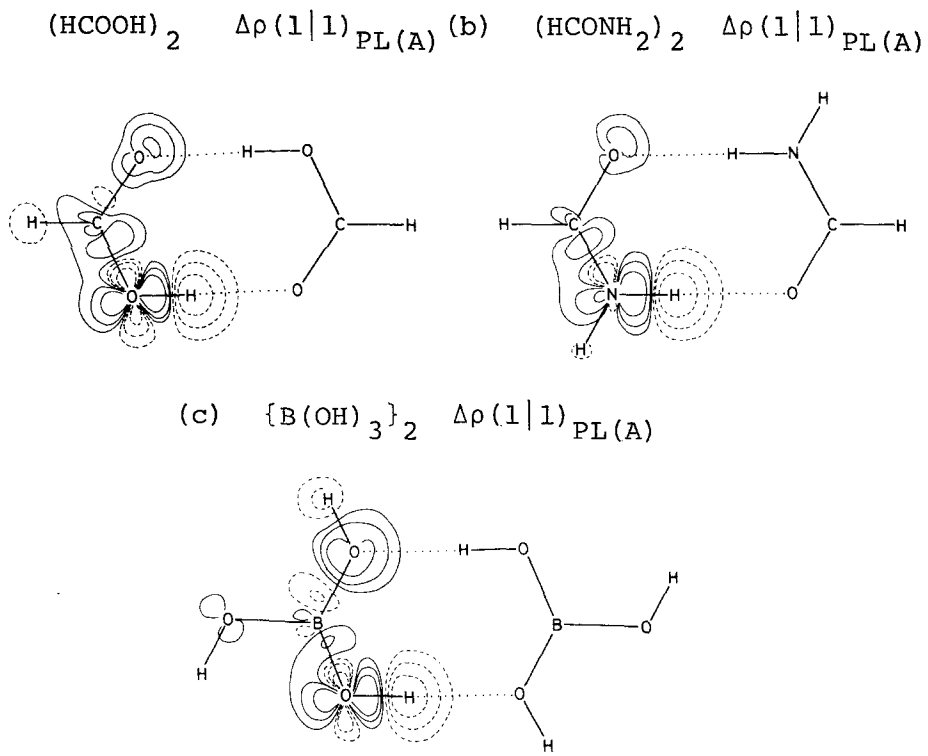

Fig. 5. The difference electron density due to the polarization interaction in $(HCOOH)_2$, $(HCONH_2)_2$ and $(B(OH)_3)_2$. See Fig. 2 for detail

11(σ), 12(π), 25(π^*), 26(σ^*) and 27(σ^*) MO's from the monomer A and 22(σ), 23(σ), 24(π), 30(π^*), 31(σ^*) and 32(σ^*) from B as such active MO's. The shape of the spatial extension of these six MO's of A is roughly sketched in Fig. 8. In this figure, one can see that the combination of the 10th and 11th σ MO's yields a favorable orbital for the CT interaction along the H-bond. Through the mixing of these two, the carbonyl oxygen gets the sp^2 like orbital which is effective to attack the O–H σ^* antibonding orbital. Similarly through the mixing of 31st and 32nd σ^* MO's, proton gains the large lobe of the unoccupied orbital waiting for the jumping-in of electrons from the carbonyl sp^2 lone-pair orbital. In order to examine the contribution of these twelve MO's to E_{EX}, E_{PL} and E_{CT}, we recalculate these three terms. They are shown in Table 4. These values which are part of those in Table 1 tell us to what extent the particular orbital interaction by these twelve MO's contributes to each energy term. In this table, E_{EX}^{σ}(partial) is the exchange energy due to overlap of the σ-type (10th, 11th, 22nd and 23rd) MO's and is calculated to be 6.57 kcal/mole. On the other hand, E_{EX}^{π}(partial) is originating from the overlap between the 12th MO of A and the 24th MO of B and is found to be almost zero. Referring to the global E_{EX} (22.94 kcal/mole) of $(HCOOH)_2$ in Table 1, one can see that the exchange energy is not recovered by MO pairs selected now. This suggests that E_{EX} is composed of all the combinations of occupied MO

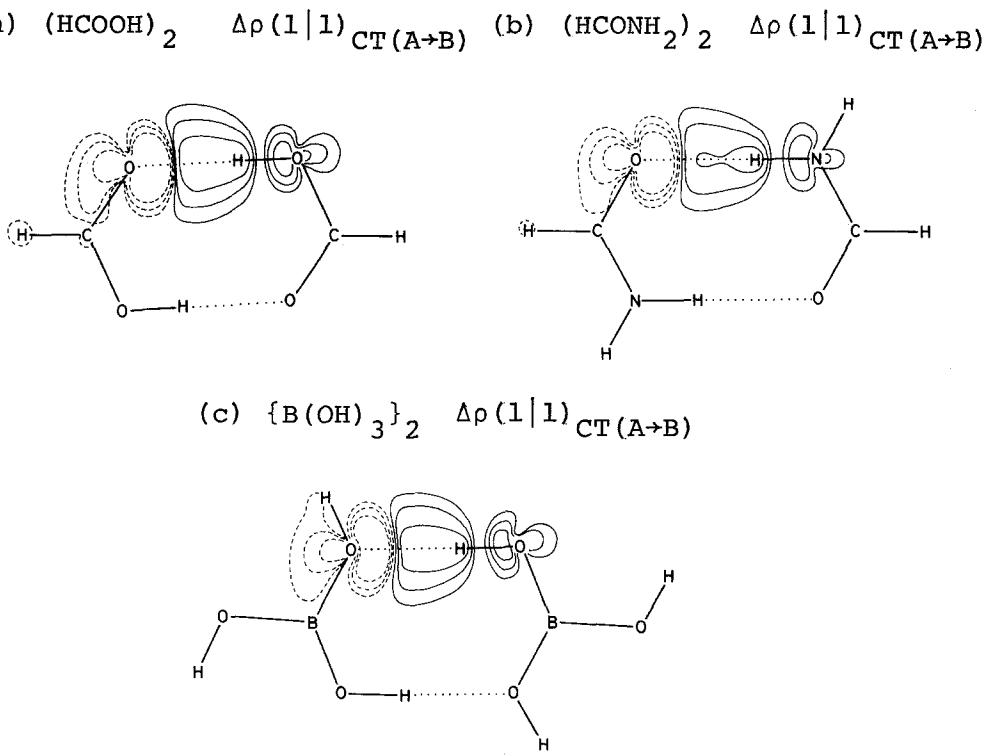

Fig. 6. The difference electron density due to the charge-transfer interaction in $(HCOOH)_2$, $(HCONH_2)_2$ and $(B(OH)_3)_2$. See Fig. 2 for detail

pairs for which the weight of the contribution to the energy is appreciably averaged. On the other hand, E_{CT}^{σ} (partial) $+E_{CT}^{\pi}$ (partial) can substantially reproduce the global E_{CT} (-20.56 kcal/mole) in Table 1. While E_{CT}^{π}(partial) is almost zero, E_{CT}^{σ}(partial) is calculated to be -15.00 kcal/mole. This indicates that the CT interaction between two σ-type occupied MO's of A and two σ-type unoccupied ones of B and *vice versa* is overwhelmingly important. The nature of this particular CT interaction is really in contrast to the distributed manner of the exchange interaction. With the satisfactory reliability, one can describe the CT energy in terms of these particular combinations of σ and σ^* MO's. The polarization term, E_{PL}^{σ}(partial) $+E_{PL}^{\pi}$(partial), is also found to be a good approximation to the global E_{PL} (-0.84 kcal/mole) in Table 1. Contrary to the cases of exchange and CT energies, E_{PL}^{π}(partial) is larger (absolute value) than E_{PL}^{σ}(partial). This result is reasonable, because π electrons are more easily moved by the approach of the external polar species than σ electrons. This mobility of the former electrons gives the serious change of the charge distribution which is already examined by the Mulliken population analysis. Reviewing the results of exchange, CT and polarization terms, one realizes that the selection of six "active" MO's of each monomer is reasonable to detect the main source of E_{CT} and E_{PL} but reproduces only a small portion of E_{EX}. The success of this selection in describing E_{CT} and E_{PL}

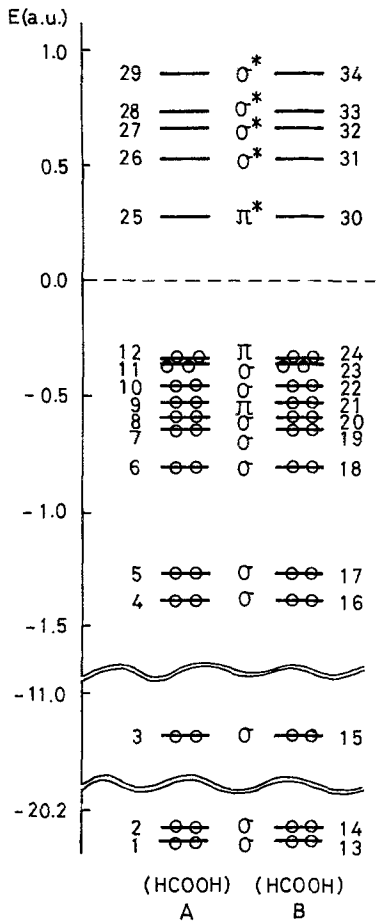

Fig. 7. The orbital energy of the HCOOH monomer calculated with the STO-3G minimal basis. The number attached to each MO runs ($1 \rightarrow 12$, $25 \rightarrow 29$) in A and it runs ($13 \rightarrow 24$, $30 \rightarrow 34$) in B. σ and σ^* indicates the MO in the x-z plane of Fig. 1, π and π^* show the MO along the y axis

and the failure in E_{EX} are explainable from the point of view of the perturbation theory. The former two energies are of the second order in the sense of Rayleigh–Schroedinger perturbation theory. The denominator of their expression has the gap of orbital energies between occupied and unoccupied MO's. Since the present choice of six active MO's is based solely on the height of the orbital energy, they can give the small value of denominators and consequently magnify the particular components of E_{CT} and E_{PL}. On the other hand, the exchange energy is of the first order and is independent of the orbital energy. Thus, the small value of E_{EX}^{σ}(partial) is understandable.

The contribution of four active (two occupied and and two unoccupied) σ MO's of A and B to the interaction energy has been investigated energetically. In order to see their role on the charge redistribution of $(HCOOH)_2$, three difference density maps including the above mentioned particular exchange, polarization and CT interactions are drawn in Figs. 9a, 9b and 9c, respectively. In Fig. 9a, the minor change of the charge distribution due to the particular exchange interaction is

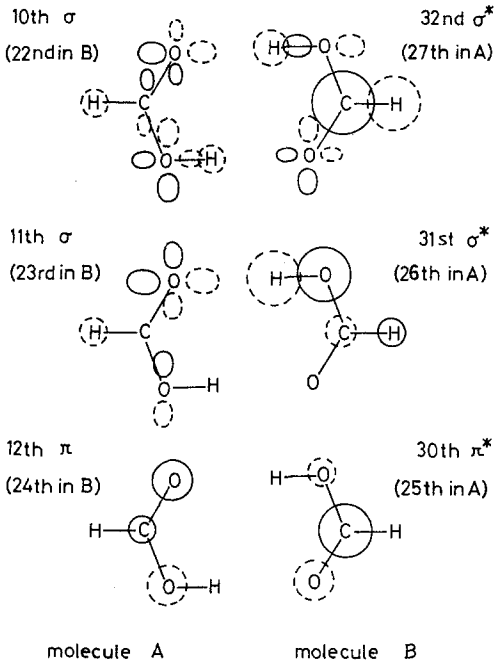

Fig. 8. Rough sketch of the six "active" MO's of HCOOH. The circle of the full line has the opposite sign of the coefficient against that of the dotted line

demonstrated, although the trend of the change is in line with that of the global exchange interaction shown in Fig. 2b. As anticipated from the small value (6.57 kcal/mole) of E_{EX}^{σ}(partial) $+E_{EX}^{\pi}$(partial), the effect of the partial exchange interaction on the electron movement is not significant. In Fig. 9b, the difference density map due to the particular polarization interaction exhibits a smaller charge redistribution than that due to the global polarization interaction in Fig. 2c. This result indicates that the σ polarization is not so drastic. In Fig. 9c, the difference density map due to the particular CT interaction shows a considerable electron migration from A to B, and the extent of the change covers almost that of the global CT interaction shown in Fig. 2d. Therefore, it is again affirmed by this figure that the choice of four active σ MO's of A and B is a valid way to describe the greater part of the net CT interaction. But there is a notable difference between Fig. 2d and Fig. 9c on the terminal hydrogen and the hydroxyl group A. The

Component	Energies
E_{EX}^{σ}(partial)	6.57
E_{EX}^{π}(partial)	0.00
E_{PL}^{σ}(partial)	−0.16
E_{PL}^{π}(partial)	−0.48
E_{CT}^{σ}(partial)	−15.00
E_{CT}^{π}(partial)	−0.00

Table 4. The partial interaction energies of $(HCOOH)_2$ in the frame of the six (A) and six (B) active MO's shown in Fig. 8. All values are in kcal/mole and their negative ones denote the stabilization energies

(a) $(HCOOH)_2$ $\Delta\rho(1|1)^{\sigma}_{EX}$(partial)

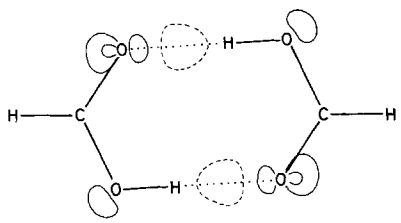

(b) $(HCOOH)_2$ $\Delta\rho(1|1)^{\sigma}_{PL(A)}$(partial)

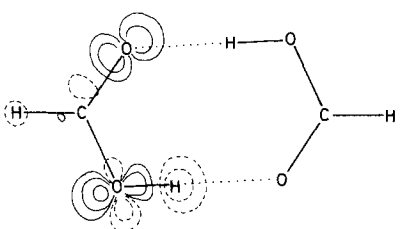

(c) $(HCOOH)_2$ $\Delta\rho(1|1)^{\sigma}_{CT(A\rightarrow B)}$(partial)

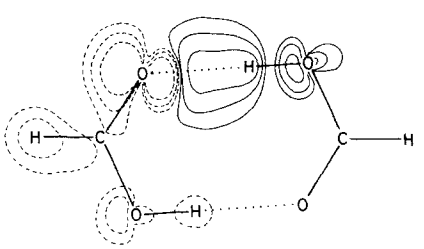

Fig. 9. The difference electron density due to the particular MO–MO interaction in $(HCOOH)_2$. See Fig. 2 for detail

moderately decreased density on these atoms is observed in the latter figure, whereas it is negligible in the former figure. This density at the non-H-bonded area reflects the nature of MO's which make electrons delocalized over the entire system. Since the density map in Fig. 9c is drawn by the use of only two occupied σ MO's of A, the superposition of them cannot describe the localized orbital along the H-bond quite well (see Fig. 8).

5. Conclusive Discussion

In this work, the nature of the two H-bonds, of the cyclic dimer is elucidated in terms of various types of electronic interaction. The energy decomposition scheme

which is a useful means to shed light on the intermolecular interaction is applied to three cyclic dimers, $(HCOOH)_2$, $(HCONH_2)_2$ and $(B(OH)_3)_2$. The detailed analysis of the interaction energy (ΔE) and its corresponding density redistribution, $\Delta\rho(1 \mid 1)$, is made with respect to the $(HCOOH)_2$ system.

Firstly, the validity of the present definition of E_{PL} and E_{CT} is demonstrated. That is, as for the polarization, the coupling term between the two one-sided polarizations can be neglected and consequently the one-sided polarization can be treated independently within each monomer. Thus, E_{PL} is twice as large as the one-sided polarization in such a weak interacting system as $(HCOOH)_2$. Similarly, the effect of the mutual CT (i.e., coupling between donation and back donation) can be omitted with the sufficient accuracy.

The charge redistribution of σ electrons shows the characteristic role of each component of $\Delta\rho(1 \mid 1)$ which is almost the same as is obtained in such a system of the single O···H–O bond as $(H_2O)_2$. But, some noticeable points of the cyclic dimer are clarified here. While $\Delta\rho(1 \mid 1)_{EX}$ and $\Delta\rho(1 \mid 1)_{CT}$ exhibit the locality of the charge redistribution around the O···H–O and O–H···O regions, $\Delta\rho(1 \mid 1)_{PL}$ and $\Delta\rho(1 \mid 1)_{MIX}$ show the widely spread charge alternation along the intramolecular bonds. These two interactions cause the gathering of the density of the mobile π electrons on to the carbonyl oxygen atom (see Table 3). In particular, the polarization interaction operates to connect (or couple) two H-bonds effectively in spite of the small energy component, E_{PL}. The comparison of five components of ΔE between $(HCOOH)_2$ and $(HCONH_2)_2$ reveals the clear difference, although the global ΔE's are apparently almost the same. A dimer system, $(B(OH)_3)_2$, shows the complex charge redistribution which promotes the H-bond formation with the neighboring four $B(OH)_3$'s around the dimer.

The energy decomposition scheme is discussed in terms of the orbital interaction. The contribution of some particular combination of MO's to E_{EX}, E_{PL}, and E_{CT} is examined. Then, the present choice of four "active" σ MO's from both monomers is found to reproduce the appreciable part of E_{CT} and the corresponding $\Delta\rho(1 \mid 1)_{CT(A\rightarrow B)}$, which supports the usefulness of the frontier electron theory of Fukui [25] as to the chemical reactivity. While E_{PL} and $\Delta\rho(1 \mid)_{PL(A)}$ are moderately reproduced, only a small portion of E_{EX} and $\Delta\rho(1 \mid 1)_{EX}$ is recovered by that selection of MO's. Since the exchange energy which is of the first order in the perturbation expansion does not have the orbital energy dependence, E_{EX} cannot be recovered by E_{EX}(partial).

Since such an analysis of the particular orbital interaction as is made here can be straightforwardly applied to any type of the H-bonded system, the study of the energy decomposition scheme in the MO language seems a promising approach to the unified interpretation of that system.

Acknowledgements. We are grateful to Professor Keiji Morokuma who kindly gave the revised FORTRAN program of GAUSSIAN 70 to one of the authors (S.Y.). Thanks are due to Professor Kenichi Fukui for his instructive guidance to the orbital interaction concept. Also, we would like to express our gratitude to the Data Processing Center, Kyoto University, for its generous permission to use the FACOM 230-75 computer.

References

1. Kollman, P. A., Allen, L. C.: Chem. Rev. **72**, 283 (1972)
2. Van Duijneveldt, F. B., Murrell, J. N.: J. Chem. Phys. **46**, 1759 (1967)
3. a) Kollman, P. A., Allen, L. C.: Theoret. Chim. Acta (Berl.) **18**, 399 (1970)
   b) Dreyfus, M., Pullman, A.: Theoret. Chim. Acta (Berl.) **19**, 20 (1970)
   c) Morokuma, K.: J. Phys. Chem. **55**, 1236 (1971)
4. Morita, H., Nagakura, S.: Theoret. Chim. Acta (Berl.) **27**, 325 (1972)
5. Kitaura, K., Morokuma, K.: Intern. J. Quantum Chem. **10**, 325 (1976)
6. Umeyama, H., Morokuma, K.: J. Am. Chem. Soc. **98**, 7208 (1976)
7. Karle, G., Brockway, L. O.: J. Am. Chem. Soc. **66**, 574 (1944)
8. Clementi, E., Mehl, J., Von Niessen, W.: J. Chem. Phys. **54**, 508 (1971)
9. Umeyama, H., Morokuma, K.: J. Am. Chem. Soc. **99**, 1316 (1977)
10. Fukui, K., Fujimoto, H.: Bull. Chem. Soc. Japan **42**, 3399 (1969)
11. Ruedenberg, K.: Rev. Mod. Phys. **34**, 326 (1962)
12. Yamabe, S., Morokuma, K.: J. Am. Chem. Soc. **97**, 4458 (1975)
13. Ditchfield, R., Hehre, W. J., Pople, J. A.: J. Chem. Phys. **54**, 724 (1971)
14. Hehre, W. J., Lathan, W. A., Ditchfield, R., Newton, M. D., Pople, J. A.: Program number 236 distributed by the QCPE, Indiana University (1973)
15. Iwata, S., Morokuma, K.: J. Am. Chem. Soc. **95**, 7563 (1973)
16. Newton, M. D., Lathan, W. A., Hehre, W. J., Pople, J. A.: J. Chem. Phys. **52**, 4064 (1970)
17. a) Del Bene, J. E., Kochenour, W. L.: J. Am. Chem. Soc. **98**, 2041 (1976)
    b) Iwata, S., Morokuma, K.: Theoret. Chim. Acta (Berl.) **44**, 323 (1977)
18. Ladell, J., Post, B.: Acta Cryst. **7**, 559 (1954)
19. Dreyfus, M., Maigret, B., Pullman, A: Theoret. Chim. Acta (Berl.) **17**, 109 (1970)
20. Craven, B. M., Sabine, T. M.: Acta Cryst. **20**, 214 (1966)
21. Lerner, R. G., Friend, J. P., Dailey, B. P.: J. Chem. Phys. **23**, 201 (1955)
22. Clague, A. D. H., Bernstein, J. H.: Spectrochim. Acta, part A **25**, 593 (1969)
23. Fukui, K., Fujimoto, H.: Bull. Chem. Soc. Japan **41**, 1989 (1968)
24. Bonaccorsi, R., Petrongold, C., Scrocco, E., Tomasi, J.: Theoret. Chim. Acta (Berl.) **20**, 331 (1971)
25. Fukui, K.: Fortschr. Chem. Forsch. **15**, 1 (1970)

Received May 11, 1977/August 31, 1977